

Theoretical study on windage loss characteristics of supercritical carbon dioxide in a rotating annular gap

Buze Chen'

Master Student

School of Engineering Science, University of
Chinese Academy of Sciences;
Key Laboratory of Advanced Energy and Power,
Institute of Engineering Thermophysics, Chinese
Academy of Sciences,
Beijing, China

Chaohong Guo*

Associate Research Fellow

School of Engineering Science, University of
Chinese Academy of Sciences;
Key Laboratory of Advanced Energy and Power,
Institute of Engineering Thermophysics, Chinese
Academy of Sciences,
Beijing, China

Fengxiang Lu

PhD Student

School of Engineering Science, University of
Chinese Academy of Sciences;
Key Laboratory of Advanced Energy and Power,
Institute of Engineering Thermophysics, Chinese
Academy of Sciences,
Beijing, China

Yuming Zhu

Assistant Research Fellow

School of Engineering Science, University of
Chinese Academy of Sciences;
Key Laboratory of Advanced Energy and Power,
Institute of Engineering Thermophysics, Chinese
Academy of Sciences,
Beijing, China

Shiqiang Liang

Associate Research Fellow

School of Engineering Science, University of
Chinese Academy of Sciences;
Key Laboratory of Advanced Energy and Power,
Institute of Engineering Thermophysics, Chinese
Academy of Sciences,
Beijing, China

Bo Wang

Associate Research Fellow

School of Engineering Science, University of
Chinese Academy of Sciences;
Key Laboratory of Advanced Energy and Power,
Institute of Engineering Thermophysics, Chinese
Academy of Sciences,
Beijing, China

Xiang Xu

Director

School of Engineering Science, University of
Chinese Academy of Sciences;
Key Laboratory of Advanced Energy and Power,
Institute of Engineering Thermophysics, Chinese
Academy of Sciences,
Beijing, China

ABSTRACT

In the realm of Supercritical Carbon Dioxide (S-CO₂) rotary machinery, a shaft-type clearance is formed between the rotating rotor and stationary casing—a phenomenon prevalent in electric motors, compressors, and turbines. Due to its high density, the rotational flow of S-CO₂ within such clearances results in significant windage loss, exerting a substantial impact on the performance of rotary machinery. Addressing this issue, this paper employs numerical simulation to theoretically investigate the aerodynamic drag characteristics induced by high-speed rotation of S-CO₂ within shaft-type clearances.

* Corresponding author

Initially, the numerical calculation method is validated using experimental data from existing literature. Subsequently, an analysis is conducted on the influences of flow parameters and geometric structures on the characteristics of windage loss. This includes an examination of various flow field features such as temperature distribution, pressure distribution, and velocity distribution, along with an assessment of the applicability of Taylor vortex transition points and existing correlations. The results indicate that an increase in S-CO₂ density leads to higher wall shear forces and elevated temperature rise. The fluctuation in radial velocity corresponds well with Taylor vortex transition, and the windage loss is found to be adequately described by the established correlation for TCP flow.

INTRODUCTION

The As society rapidly advances, the escalating conflict between energy and the environment has become increasingly severe. Supercritical carbon dioxide (S-CO₂) Brayton cycle power generation technology, with its excellent environmental-friendly characteristics, has gradually become a research hotspot. Unlike traditional power generation systems using steam as the working fluid, S-CO₂ power generation technology utilizes the characteristics of supercritical fluids, addressing issues such as high compression power consumption and low thermal efficiency[1]. However, as research progresses, experimental setups established by various institutions have encountered significant windage loss issues, directly leading to research stagnation. Representative examples include the Sandia National Laboratories in the United States [2], the BMPC Laboratories in the United States[3,4], and the IAE Institute in Japan[5]. The root cause of this problem lies in the gaps between impellers and seals, stators and shafts in critical components of systems such as motors, compressors, and turbines, which are filled with S-CO₂. Due to the higher density of S-CO₂ compared to air or steam, coupled with high rotational speeds of the units, substantial windage loss has been generated[6-8].

The windage loss generated by rotational flow is typically calculated using the following equation:

$$W = \pi\rho C_f R_1^4 \omega^3 L \quad (1)$$

where ρ is the fluid density (kg/m³), R_1 is the radius within the gap, i.e., the rotor radius (m), ω is the angular velocity (rad/s), and L is the axial length (m). C_f is the surface friction coefficient, an empirical factor introduced for improved calculation accuracy. Previous research has indicated that windage loss in TC flow can be predicted using this correlation equation. Various models exist for predicting, applicable under different conditions [9-15]. Most existing literature focuses on flow losses within the enclosed air in motor cavities, primarily addressing air TC flow [16-21]. Research on TC flow for S-CO₂ occasionally appears [9, 22], but studies on TCP flow are scarce, especially lacking in research on S-CO₂ TCP flow. To break through S-CO₂ turbine design technology and enhance equipment performance, in-depth research on wind-induced windage loss in S-CO₂ TCP flow is urgently needed. Against this background, this paper conducts a series of studies on flow field characteristics (temperature field, pressure field, velocity field), Taylor vortex transition points, and the applicability of existing correlation equations.

METHODOLOGY

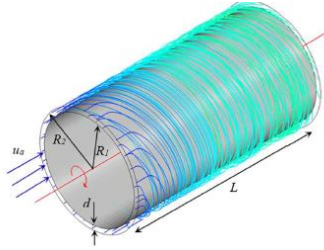


Fig. 1 Geometric model of TCP flow

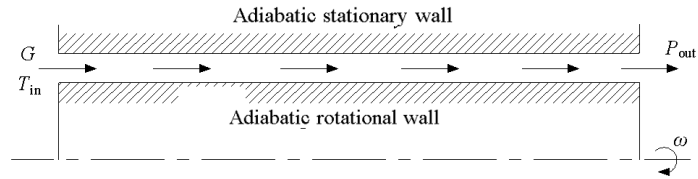


Fig. 2 Numerical simulation computing domain

The basic geometric model of the TCP flow is illustrated in [Figure 1](#), where R_1 represents the rotor radius, R_2 represents the stator radius, L represents the axial length, and d represents the gap width, which is equal to $R_2 - R_1$. The three-dimensional numerical simulation domain is depicted in [Figure 2](#), with mass flow rate and temperature boundaries at the inlet and pressure boundary at the outlet. Additionally, based on the TCP flow model, wall conditions are set with the inner wall rotating and the outer wall stationary. To better investigate the characteristics of windage loss, both conditions are considered adiabatic.

To validate the computational method, the windage loss experimental data of air obtained by Anderson [23] using the force balance method is compared with the CFD results in this study. The literature focuses on a high-speed motor as the experimental subject, with axial airflow in the annular gap between the motor stator and rotor, forming an air TCP flow. The dimensions and relevant boundary conditions for the experiment are presented in [Table 1](#).

Table 1 Model size and boundary parameters used in case verification [19]

Parameter	Value	Unit
Rotor radius R_1	43.5	mm
Stator radius R_2	45.5	mm
Gap width δ	2	mm
Axial length L	60	mm
Inlet flow rate G	0.00373	kg/s
Inlet temperature T_{in}	295	K
Outlet pressure P_{out}	0.1	MPa
Rotational speed n	5000-36000	r/min

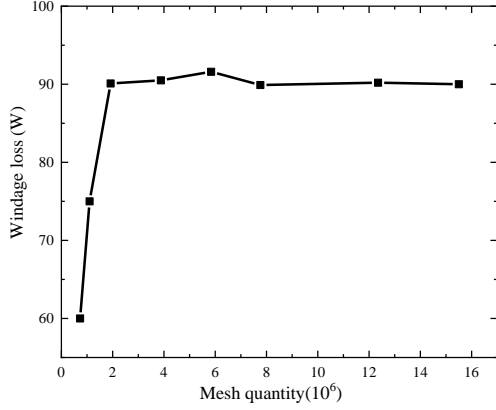


Fig. 3 Grid independence verification

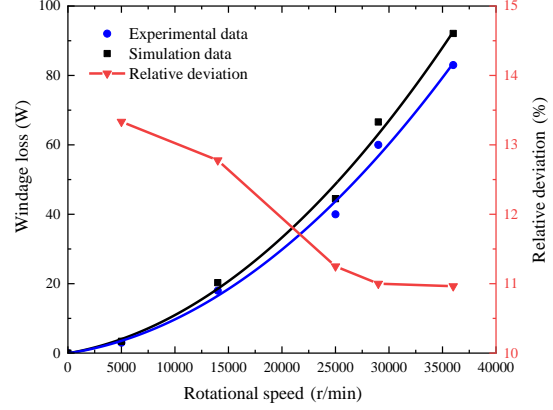


Fig. 4 Comparison between simulation results and experimental data

The simulation utilized the SST turbulence model and underwent grid independence verification. The comparison between numerical and experimental results is illustrated in Figure 4, where the horizontal axis represents the rotational speed, and the vertical axis represents the windage loss. As shown in the graph, the numerical calculation results are slightly higher than the measured data. This discrepancy could be attributed to the fact that, during the experiment, the stator and rotor were not under adiabatic conditions, leading to some error in the torque calculated using the force balance method. The relative error decreases as the rotational speed increases, with a maximum relative error of 13%. Therefore, this computational method can accurately predict the windage loss characteristics in the annular gap.

After verifying the accuracy of the model, the study in this paper investigates the following operating conditions: (1) Keeping the same boundary conditions and structural parameters, only the working fluid density is changed. (2) Keeping the same boundary conditions and structural parameters, only the rotational speed is changed. (3) Keeping the same flow parameters and structural parameters, either R_2 or R_1 is modified. The flow parameters mentioned include the rotational Reynolds number Re_v and axial Reynolds number Re_a , while the structural parameters involve the radius ratio η and the aspect ratio Γ .

$$Re_v = R_1 \frac{(R_2 - R_1)\omega\rho}{\mu} \quad (2)$$

$$Re_a = \frac{u_a * 2 * (R_2 - R_1)}{\nu} \quad (3)$$

$$\eta = \frac{R_2 - R_1}{R_1} \quad (4)$$

$$\Gamma = \frac{L}{(R_2 - R_1)} \quad (5)$$

RESULTS AND DISCUSSION

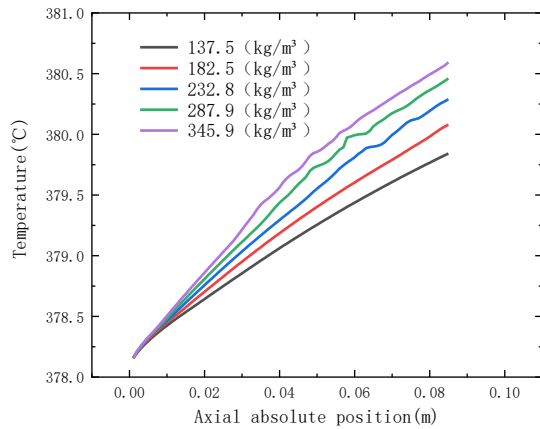


Fig.5 The temperature of the working fluid varies along the axial position at different densities

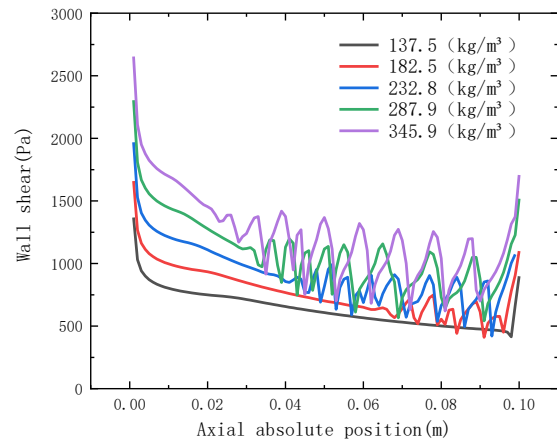


Fig.6 The wall shear varies along the axial position at different densities

From [Figure 5](#), it can be observed that the fluid temperature gradually increases with the increase in flow length. This indicates that under the action of rotor rotation, significant viscous losses occur within the fluid, leading to a gradual temperature rise. On the other hand, with an increase in working fluid density, the temperature rise becomes more pronounced. Additionally, [Figure 6](#) reveals that the wall shear force exhibits noticeable fluctuations due to the vortices generated by rotation. Moreover, as the density increases, the fluctuations in wall shear force become more significant, with higher values. This, to some extent, increases the frictional losses on the rotor surface, providing additional support to the findings in [Figure 5](#).

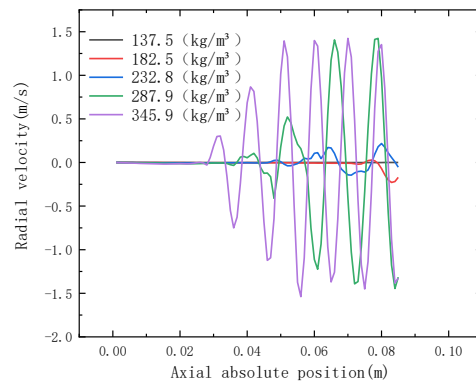


Fig.7 The radial velocity varies along the axial position at different densities

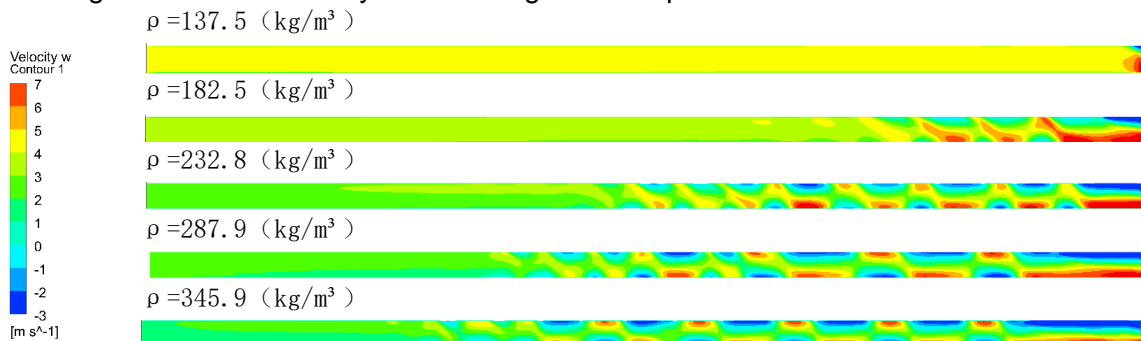


Fig.8 Axial velocity contour of an axial cross-section

Figure 7 depicts the variation curve of radial velocity along the axial position. When the density is low, it almost forms a straight line without any fluctuations. As the density increases, the starting point of the fluctuations moves closer to the inlet position, and the amplitude of the fluctuations increases. This pattern is consistent with the variation observed in the Taylor vortex transition point in the velocity contour plot (Figure 8). Further observation reveals that the starting point of the radial velocity fluctuations corresponds to the transition point of the Taylor vortices in the contour plot. This suggests that the starting point of radial velocity fluctuations can be used as a reliable indicator for determining the initiation position of Taylor vortex transition points, which is more dependable than observation in the velocity contour plot.

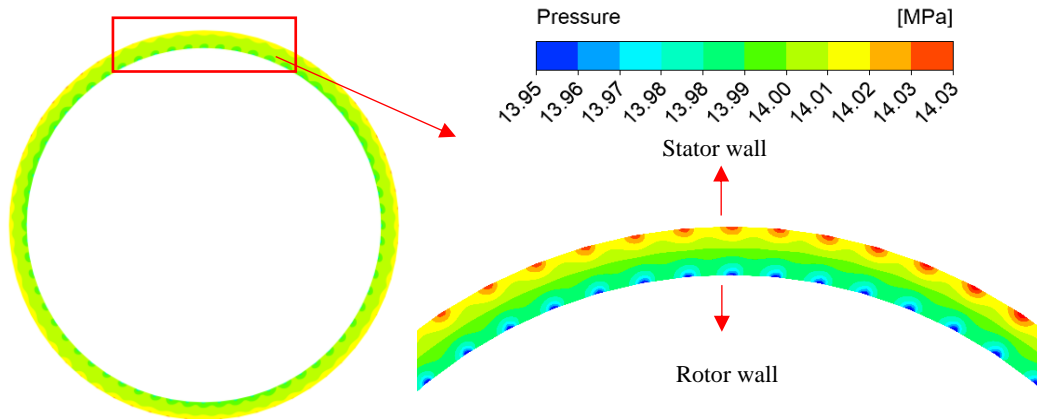
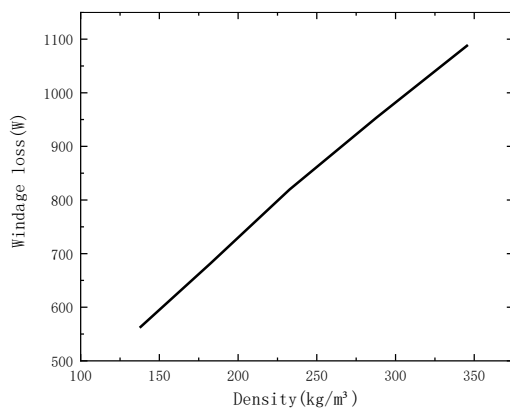
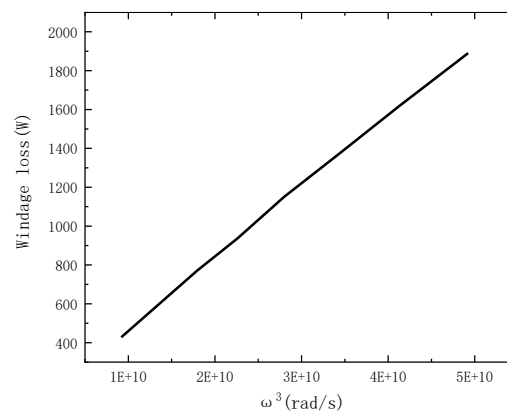


Fig.9 Pressure distribution in the tangential profile

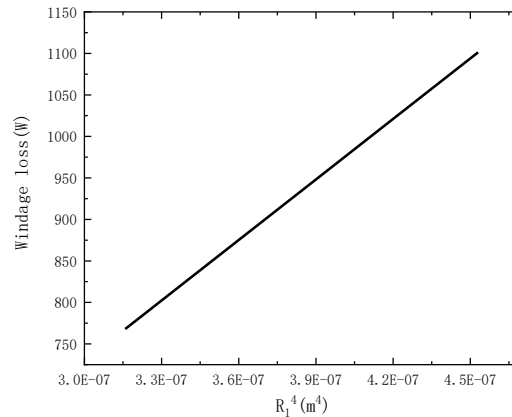
From Figure 9, it is evident that there are periodic high-pressure regions near the stator wall and periodic low-pressure regions near the rotor wall. This phenomenon occurs because the fluid on the rotor surface, under the influence of centrifugal force, accelerates and flows towards the stationary wall. As it reaches the nearly stationary wall, the velocity decreases, leading to higher stagnation pressure. The high pressure near the nearly stationary wall drives the fluid to flow back towards the rotor surface, forming the Taylor vortices.



(a) The effect of ρ on the windage loss



(b) The effect of ω^3 on the windage loss



(c) The effect of R_1^4 on the windage loss

Fig.10 Verification diagram of the applicability of the windage loss correlation formula

From the above figure, it is clear that ρ 、 ω^3 and R_1^4 are roughly linearly related to windage loss. The slight fluctuations are attributed to uncertainties in the friction coefficient, which is not discussed in this study.

In summary, an increase in S-CO₂ density results in increased wall shear force, leading to a rise in temperature. As density increases, the starting point of the radial velocity fluctuation is closer to the inlet position, aligning closely with the transition point of Taylor vortices. The basic correlation equation for windage loss is also applicable to TCP flow, though further research is needed to develop a more accurate empirical correlation for the friction coefficient.

REFERENCES

- [1] J. Xue, X.H. Nie, L. Zhao, R.K. Zhao, J.J. Wang, C.D. Yang, A.F. Lin, Molecular dynamics investigation on shear viscosity of the mixed working fluid for supercritical CO₂ Brayton cycle, *J. Supercrit. Fluids* 182 (2022), 105533. <https://doi.org/10.1016/j.supflu.2022.105533>.
- [2] Shen, G.; Yao, J.; Lou, W.; Chen, Y.; Guo, Y.; Xing, Y. An experimental investigation of streamwise and vertical wind fields on a typical three-dimensional hill. *Appl. Sci.* 10.4(2020):1463. <https://doi.org/10.3390/app10041463>.
- [3] Conboy, T.; Wright, S.; Pasch, J.; Fleming, D.; Rochau, D.; Fuller, R. Performance characteristics of an operating supercritical CO₂ Brayton cycle. *Journal of Engineering for gas turbines and power.* 2012, 134, 11-17. <https://doi.org/10.1115/1.4007199>.
- [4] Kenneth J. Kimball, Eric M. Clementoni. Supercritical carbon dioxide Brayton power cycle development overview, *Proceedings of ASME Turbo Exop 2012,6(2012),11-15*, Copenhagen, Denmark. <https://doi.org/10.1115/GT2012-68204>.
- [5] E.M.Clementoni, T.L.Cox, M.A.King. Off-nominal component performance in a supercritical carbon dioxide Brayton cycle, *Journal of Engineering for gas turbines and power*, 2016,2(138):011703. <https://doi.org/10.1115/1.4031182>. [4] Jiang J, Liang S, Xu X, et al. Experimental Research on a New Mini-Channel Transcritical CO₂ Heat Pump Gas Cooler. *Micromachines*: MDPI AG, 2023: 1094.
- [6] Guo, Jia-Qi, et al. A systematic review of supercritical carbon dioxide (S-CO₂) power cycle for energy industries: Technologies, key issues, and potential prospects. *Energy Conversion and Management* 258 (2022): 115437. <https://doi.org/10.1016/j.enconman.2022.115437>.
- [7] Quiban, R.; Changenet, C.; Marchesse, Y.; Ville, F. Experimental investigations about the power loss transition between churning and windage for spur gears. *J. Tribol.* 143(2020):024501. <https://doi.org/10.1115/1.4047949>.

- [8] Zhao, Z.; Song, W.; Jin, Y.; Lu, J. Effect of rotational speed variation on the flow characteristics in the rotor-stator system cavity. *Appl. Sci.* 2021, 11(22), 11000. <https://doi.org/10.3390/app112211000>.
- [9] SAARI, Juha, et al. Thermal analysis of high-speed induction machines. Helsinki University of Technology, 1998.
- [10] Wendt, V. Turbulente strömungen zwischen zwei rotierenden konaxialen zylinder. *Ingenieur-Archiv* 1933, 4, 577–595.
- [11] E. Bilgen, R. Boulos, Functional dependence of torque coefficient of coaxial cylinders on gap width and Reynolds numbers, *J. Fluid. Eng.* 95 (1973) 122–126.
- [12] Nakabayashi K, Yamada Y and Kishimoto T 1982 Viscous frictional torque in the flow between two concentric rotating rough cylinders *Journal of Fluid Mechanics* 119 409-422.
- [13] J.E. Vrancik, Prediction of Windage Power Loss In Alternators, NASA, US, 1968.
- [14] K. Nakabayashi, Y. Yamada, T. Kishimoto, “Viscous frictional torque in the flow between two concentric rotating rough cylinders”, *Journal of Fluid Mechanics*, vol. 119, pp. 409-422, 1982.
- [15] M. Mack, Luftreibungsverluste bei elektrischen Maschinen kleiner Baugröße. PhD thesis, Universität Stuttgart (FH), Stuttgart, 1967. [16] Motoaki Utamura, Hiroshi Hasuike, Kiichiro Ogawa, Takashi Yamamoto, Toshihiko Fukushima, Toshinori Watanabe, Takehiro Himeno. Demonstration of supercritical CO₂ closed regenerative Brayton cycle in a bench scale experiment, *Proceedings of ASME Turbo Expo 2012*, 6(2012).11-15, Copenhagen, Denmark. <https://doi.org/10.1115/GT2012-68697>.
- [17] Caobing Wei, Yang Xuc , Kai Zhangc. Research on windage losses of smooth rotor supported by active magnetic bearings in a vacuum chamber[J]. *Vacuum*,159(2019),76-81. <https://doi.org/10.1016/j.vacuum.2018.10.006>.
- [18] K. Kiyota, T. Kakishima, A. Chiba, Estimation and comparison of the windage loss of a 60 kW switched reluctance motor for hybrid electric vehicles, in: *Proc[J]. The 2014 International Power Electronics Conference*, 18–21. <https://doi.org/10.1109/IPEC.2014.6870001>.
- [19] BURNAND, Guillaume, et al. Validation by measurements of a windage losses model for very-high-speed machines. In: *2017 20th International Conference on Electrical Machines and Systems (ICEMS)*. IEEE, 2017. p. 1-4. <https://doi.org/10.1109/ICEMS.2017.8056273>.
- [20] F. Asami, M. Miyatake, S. Yoshimoto, E. Tanaka, T. Yamauchi, A method of reducing windage power loss of a high-speed motor using a viscous vacuum pump, *Precis. Eng.* 48 (2017) 60–66. <https://doi.org/10.1016/j.precisioneng.2016.11.005>.
- [21] M. Liu, W. Sixel, H. Ding, B. Sarlioglu, Investigation of rotor structure influence on the windage loss and efficiency of FSPM machine, in: *Proc[J]. 2018 IEEE Energy Conversion Congress and Exposition*, 2018,23–27, 2018. <https://doi.org/10.1109/ECCE.2018.8557816>.
- [22] D. sun, M. Zhou, H. Zhao, J. Liu, C.W. Fei, H. Li, Numerical and experimental investigations on windage heating effect of labyrinth seals, *J. Aerosp. Eng.* 2020,33. [https://doi.org/10.1061/\(ASCE\)AS.1943-5525.0001175](https://doi.org/10.1061/(ASCE)AS.1943-5525.0001175).
- [23] ANDERSON, Kevin R.; LIN, Jun; WONG, Alexander. Experimental and Numerical Study of Windage Losses in the Narrow Gap Region of a High-Speed Electric Motor. *Fluids*,3.1(2018):22. <https://doi.org/10.3390/fluids3010022>.

ACKNOWLEDGEMENTS

The authors gratefully acknowledge the National Natural Science Foundation of China (Grant No. 52176090).